DOI:10.1190/image2022-3745707.1

Next-generation resolution through multi-parameter FWI imaging

Tom Rayment, James McLeman, Karen Dancer, and Tim Burgess, DUG Technology*

Summary

Conventional seismic processing and imaging workflows employ a range of techniques such as deghosting, designature, and demultiple to attenuate parts of the wavefield that would otherwise degrade the final image due to the single scattering assumption used in common imaging algorithms. These processing steps can be time-consuming since they are performed in a linear fashion and require significant effort to parameterize and apply. Multi-parameter full waveform inversion (FWI) imaging offers an alternative approach by simultaneously inverting for various parameters including velocity and reflectivity using raw field data as input. This least-squares imaging solution uses primaries, multiples and ghosts to deliver higher-resolution images than traditional imaging algorithms. In this paper, we compare the reflectivity output from an FWI imaging approach against a conventional Kirchhoff 3D pre-stack depth migration (preSDM) and an image-domain least-squares reverse time migration (LS-RTM) at high frequency. We also demonstrate the fidelity of the velocity output from the simultaneous FWI imaging technique.

Introduction

The use of diving waves in FWI has become an industry-standard practice in model-building workflows as it can produce robust high-resolution models of the subsurface. However, due to geological constraints and limitations in the maximum recorded offset, the penetration depth of diving waves often does not extend to required reservoir depths. This has typically necessitated the use of residual move-out (RMO) reflection tomography to obtain the deeper model updates. Unfortunately, this approach has limited resolution, requires the raw data to be conditioned so that robust RMO picks can be obtained, and will be unreliable where the ray-based approximation fails. The inclusion of reflections in FWI is therefore an attractive alternative since it has the potential to overcome these limitations.

Incorporating reflections into FWI provides an opportunity not just to update velocity, but also to generate an interpretable product in a shorter timescale than is possible with a conventional processing and imaging workflow. FWI uses the raw field data to invert for a high-resolution image in an iterative least-squares sense that has the source signature, ghosts, and multiples removed. A common approach to achieve this is to include the reflections in a single parameter, high-frequency FWI to yield an interpretable model (Letki et al., 2019). The derivatives of which form a pseudo-reflectivity image (Kalinicheva et al., 2020; Zhang et al., 2020). While these can be useful as fast-track structural images, *a priori* assumptions about density limit their amplitude fidelity.

Separation of the kinematic and dynamic contributions of the FWI kernel can overcome this limitation, for example via joint migration inversion (JMI) (Berkhout, 2014c). Another such a method to achieve this is described by McLeman et al. (2021), and further demonstrated to high frequency by Rayment et al. (2022). This approach uses an augmented acoustic wave equation to update velocity and an AVA-related reflectivity simultaneously. The separation of the migration and tomographic terms is achieved with a wavenumber-domain preconditioner based on the scattering angle. The convergence rate of the simultaneous inversion was significantly improved, and crosstalk mitigated, by using an advanced quasi-Newton adaptive gradient optimizer. The important benefits of this approach are twofold: the derived velocity model can be used for conventional imaging purposes if required, and the intercept-reflectivity is kinematically correct with physically robust amplitudes that can be used for quantitative analysis.

In this paper, we continue the work of Rayment et al. (2022) by simultaneously inverting for velocity and the intercept-reflectivity vector using 3D TTI FWI up to frequencies of 85 Hz on a dataset from the Australian North-West Shelf.

Method

We consider a conventional towed-streamer survey located approximately 115 km northwest of Barrow Island, Australia. Localized channel features resulted in rapid, lateral velocity contrasts that conventional tomographic approaches find difficult to resolve as part of the velocity model building workflow. The acquisition was a dual-source, 8-streamer configuration with 6 km maximum offset. The initial model was built from an existing regional model and several passes of diving-wave only FWI up to a maximum frequency of 16 Hz, and maximum penetration depth of 2 km.

A moderate level of source signature variation was observed within the survey and so shot-by-shot signatures were derived through an FWI source-inversion scheme using the direct arrival. Reflection FWI was then performed using the field data as input with a 45-degree outer angle mute applied. The starting frequency was 16 Hz and 1/8 of the input shots were used. As the inversion

frequency was increased to the final 85 Hz maximum frequency, the number of input shots used was also increased until all the shots were used.

It is possible to update anisotropy as part of a simultaneous triple-parameter FWI for velocity, intercept-reflectivity, and epsilon (McLeman et al., 2022). However, in this instance the anisotropy remained fixed. Key events on the intercept-reflectivity volume can be compared to known well marker depths to update delta, if required.

Results

Figure 1 shows a depth slice comparison through the initial velocity model and the 85 Hz FWI imaging derived velocity model at 1.95 km depth. The significant increase in spatial resolution is immediately apparent, where the localized velocity anomalies are well captured by the FWI model. This has inevitably led to an improvement in structural simplicity of deeper events.

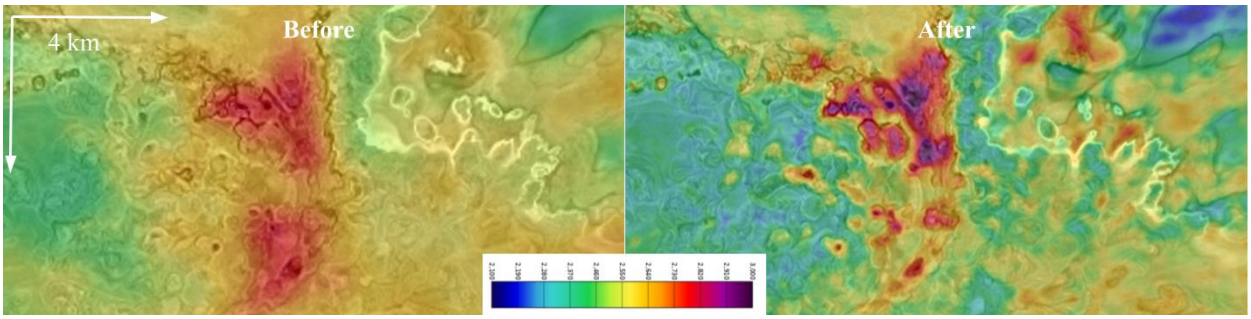

Figure 1: 2 km depth slices for (left) the initial velocity model overlain on a Kirchhoff preSDM stack and (right) the updated FWI model overlain on its corresponding Kirchhoff preSDM stack.

The impact of the improved velocity model on conventional imaging is demonstrated in Figure 2. Kirchhoff preSDM image gathers, which were generated using pre-processed data as input, demonstrate less residual RMO with the FWI updated velocity model at all depths. The stack section highlights the structural simplification of the deeper structures as a result of resolving the shallower velocity anomalies.

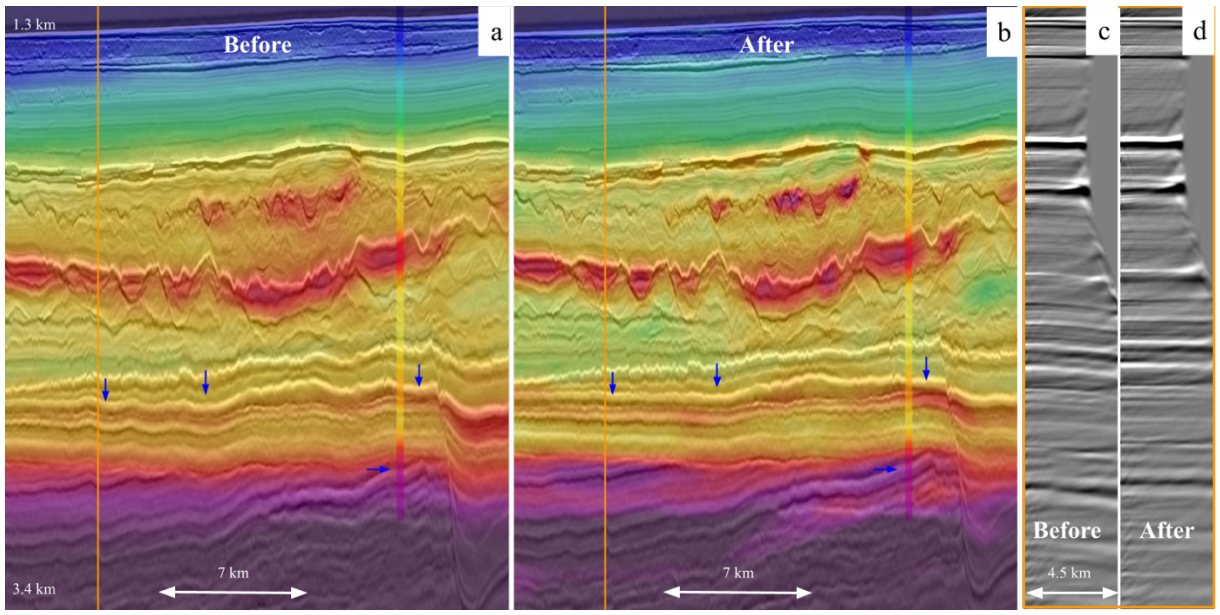

Figure 2: (a) initial FWI velocity model overlain on its Kirchhoff preSDM stack, (b) the updated FWI model overlain on its corresponding Kirchhoff preSDM stack, (c) Kirchhoff preSDM image gathers using the initial velocity, and (d) with the updated velocity.

DOI:10.1190/image2022-3745707.1

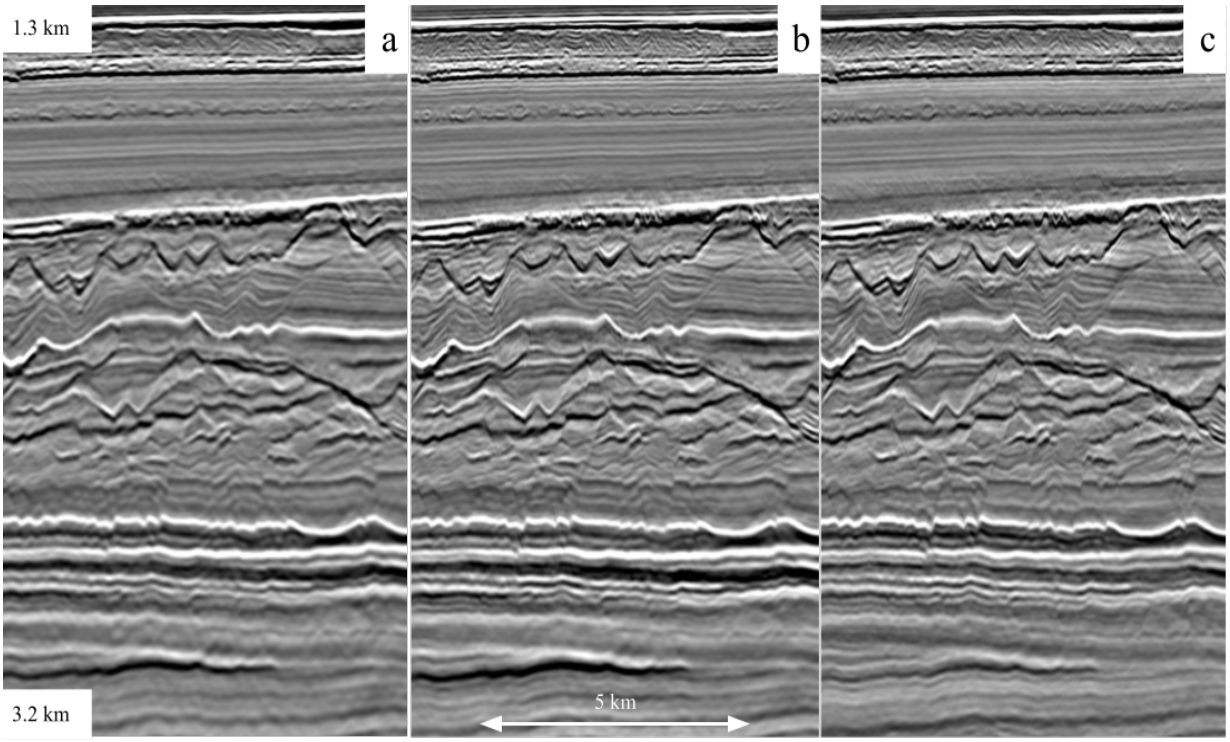

Figure 3: crossline section through (a) conventional Kirchhoff preSDM, (b) least-squares RTM, and (c) FWI derived intercept-reflectivity.

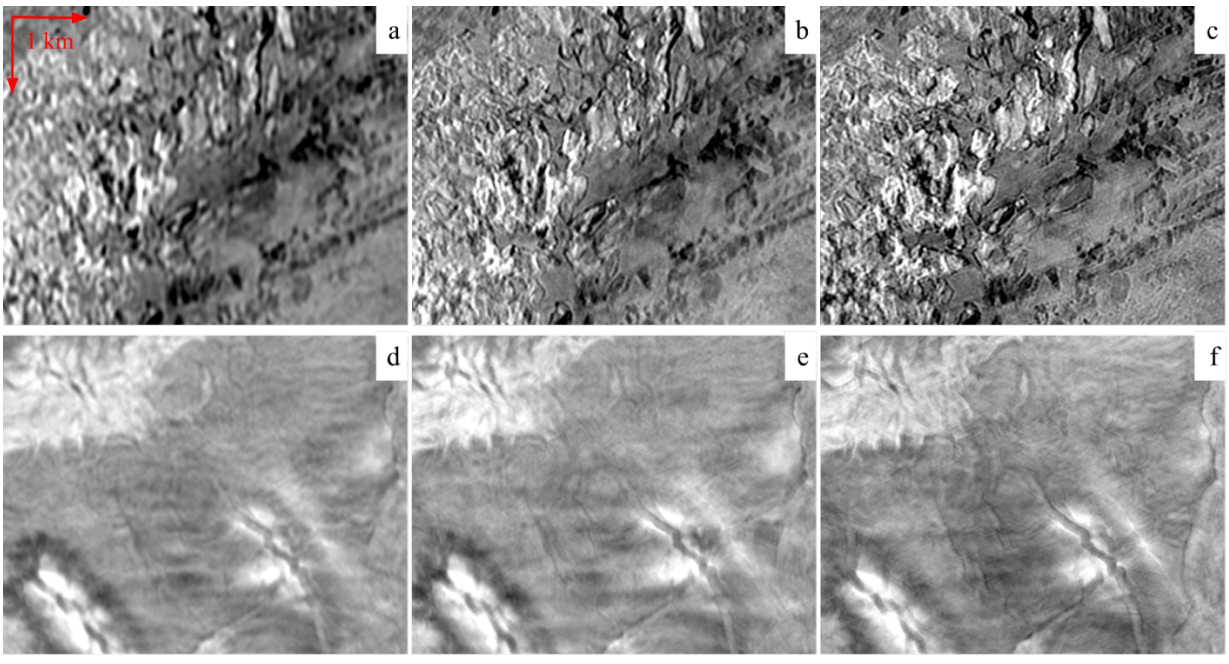

Figure 4: depth slice at 1.5 km through (a) conventional Kirchhoff preSDM, (b) least-squares RTM, and (c) FWI derived intercept-reflectivity. d), e) and f) are the same comparisons at 2.6 km depth.

Multi-parameter FWI imaging

The intercept-reflectivity is additionally output from the multi-parameter FWI imaging process and is demonstrated in Figures 3 and 4. To show the uplift, a comparison is made with more conventional imaging algorithms, i.e., Kirchhoff preSDM and an image-domain LS-RTM. To make the comparison fair, both are using processed data as input and are limited to a maximum frequency of 85 Hz. As expected, the LS-RTM shows a significant improvement in spatial resolution compared to the Kirchhoff preSDM. However, the FWI intercept-reflectivity image, which is derived by an iterative least-squares approach, has delivered a further improvement in resolution with improved structural delineation apparent in the depth and vertical sections. The FWI image, which was derived using the field data as input, shows no multiple or ghost energy leakage and is zero-phase. This demonstrates the success of the FWI imaging approach since it has successfully achieved designature, deghosting, demultiple, model building, and least-squares imaging in a single step.

To further highlight interesting geological features such as faults and channel boundaries, one can examine combinations of the components of the intercept-reflectivity vector. For example, Figure 5 shows a depth slice comparing the intercept reflectivity (left), and the horizontal reflectivity which is the norm of its horizontal components (right).

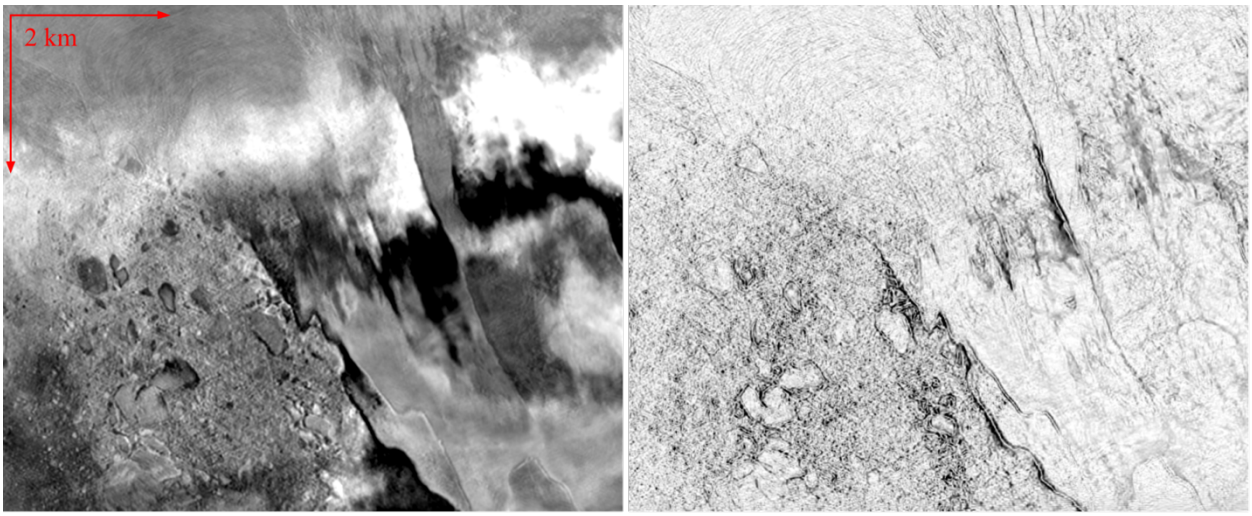

Figure 5: a depth slice at 1.8 km through (left) the intercept-reflectivity and (right) the horizontal intercept-reflectivity.

Conclusions

The novel simultaneous FWI imaging technique has demonstrated success in deriving a velocity model and intercept-reflectivity vector using primaries, ghosts, and multiples at high frequencies. Recognizing the importance of separating the kinematic and dynamic effects of the FWI kernel allows for the generation of high-resolution velocity models and an intercept-reflectivity image which presents an increase in resolution compared to both Kirchhoff preSDM and LS-RTM. Combinations of the components of the intercept-reflectivity vector can be used to gain additional insight into the subsurface by highlighting complex lateral variations in geology, such as faults and channels, which can further aid in the interpretation process.

The success of FWI imaging in handling many of the traditional processing stages such as deghosting, demultiple, and designature while simultaneously deriving a range of subsurface parameters, including velocity and intercept-reflectivity, faster than a conventional processing and imaging workflow shows the potential of this approach to supersede a conventional processing and imaging workflow.

Acknowledgements

We would like to thank Multi-Client Resources (MCR) for permission to use the BEX MC3D dataset and DUG Technology (DUG) for allowing us to present this work.

REFERENCES

Berkhout, A. J., 2014, Review paper: An outlook on the future of seismic imaging, Part III: Joint migration inversion: Geophysical Prospecting, **62**, 950–971, doi: https://doi.org/10.1111/1365-2478.12158.

Kalinicheva, T., M. Warner, and F. Mancini, 2020, Full-bandwidth FWI: 90th Annual International Meeting, SEG, Expanded Abstracts, 651–655, doi: https://doi.org/10.1190/segam2020-3425522.1.

Letki, L., M. Lamont, and T. Thompson, 2019, High frequency full waveform inversion as an interpretation solution: The APPEA Journal, **59**, 904–908, doi: https://doi.org/10.1071/AJ18123.

McLeman, J., T. Burgess, and T. Rayment, 2022, FWI imaging with simultaneous anisotropy estimation: 83rd Conference and Exhibition, EAGE, Extended Abstracts, doi: https://doi.org/10.3997/2214-4609.202210075.

McLeman, J., T. Burgess, M. Sinha, G. Hampson, and T. Thompson, 2021, Reflection FWI with an augmented wave equation and quasi-Newton adaptive gradient scheme: First International Meeting for Applied Geoscience & Energy, Expanded Abstracts, 667–671, doi: https://doi.org/10.1190/segam2021-3582659.1.

Rayment, T., K. Dancer, J. McLeman, and T. Burgess, 2022, High-resolution FWI imaging—An alternative to conventional processing: 83rd Conference and Exhibition, EAGE, Extended Abstracts, doi: https://doi.org/10.3997/2214-4609.202210233.

Zhang, Z., Z. Wu, Z. Wei, J. Mei, R. Huang, and P. Wang, 2020, FWI imaging: Full-wavefield imaging through full-waveform inversion: 90th Annual International Meeting, SEG, Expanded Abstracts, 656–660, doi: https://doi.org/10.1190/segam2020-3427858.1.